

Showcasing research from Ralf Tonner's and Johanna Heine's group, Department of Chemistry and Collaborative Research Center 1083, Philipps-Universität, Marburg, Germany. Image designed and illustrated by Leander Aurel Taubner.

Synthesis of a two-dimensional organic–inorganic bismuth iodide metalate through *in situ* formation of iminium cations

$(\text{Me}_2\text{C}=\text{NMe}_2)\text{Bi}_2\text{I}_7$  represents a new layered organic–inorganic iodido bismuthate. It displays an unprecedented anion topology, a low band gap and good stability. Advanced electronic structure analysis finds the I...I interactions to be decisive for the compound's structural and electronic properties.

As featured in:



See Ralf Tonner,  
Johanna Heine *et al.*,  
*Chem. Commun.*, 2019, 55, 14725.



Cite this: *Chem. Commun.*, 2019, 55, 14725

Received 26th August 2019,  
Accepted 26th October 2019

DOI: 10.1039/c9cc06625j

rsc.li/chemcomm

# Synthesis of a two-dimensional organic–inorganic bismuth iodide metalate through *in situ* formation of iminium cations†

Natalie Dehnhardt, Jan-Niclas Luy, Marvin Szabo, Mirco Wende, Ralf Tonner\* and Johanna Heine\*

**(Me<sub>2</sub>C=NMe<sub>2</sub>)Bi<sub>2</sub>I<sub>7</sub> represents a new layered organic–inorganic iodido bismuthate. It displays an unprecedented anion topology, a low band gap and good stability. Advanced electronic structure analysis finds the I···I interactions to be decisive for the compound's structural and electronic properties.**

Lead halide perovskites like (CH<sub>3</sub>NH<sub>3</sub>)PbI<sub>3</sub> are prominent materials due to their excellent semiconductor properties<sup>1</sup> and successful application in solar cells,<sup>2</sup> photocatalysis<sup>3</sup> and LEDs.<sup>4</sup> Layered perovskites such as (C<sub>4</sub>H<sub>9</sub>NH<sub>3</sub>)PbI<sub>4</sub><sup>5,6</sup> offer the benefit of greater stability and allow the use of larger, functional organic cations while maintaining the good semiconductor properties of their parent perovskites.<sup>7</sup> However, the toxicity of lead compounds has prompted researchers to look to related halogenido metalates for alternatives. Iodido bismuthates appear promising, as bismuth compounds are typically non-toxic.<sup>8</sup> Compounds like (CH<sub>3</sub>NH<sub>3</sub>)<sub>3</sub>Bi<sub>2</sub>I<sub>9</sub>, which features dinuclear Bi<sub>2</sub>I<sub>9</sub><sup>3-</sup> anions,<sup>9</sup> have been tested in photovoltaic devices, but only show moderate efficiencies up to 3.17% after significant efforts at optimization.<sup>10</sup> In contrast, lead halide perovskite solar cells currently reach well above 20%.<sup>11</sup> One reason for this difference in properties lies in the structural chemistry of the iodido bismuthates: while iodido plumbates readily feature layer or network anions, bismuthates are mostly limited to molecular or chain-like anions.<sup>12</sup> Only two types of iodido bismuthates with a layered anion have been reported to date: the all-inorganic family A<sub>3</sub>Bi<sub>2</sub>I<sub>9</sub> (A = K, Rb)<sup>13</sup> featuring (111) perovskite layers, and (H<sub>2</sub>AEQT)Bi<sub>2/3</sub>I<sub>4</sub> (AEQT = 5,5'''-bis-(aminoethyl)-2,2':5',2'':5'',2'''-quaterthiophene), featuring a metal-deficient (001) perovskite layer.<sup>14</sup> However, the synthesis of the layered mixed halide bismuthate (TMP)<sub>1.5</sub>[Bi<sub>2</sub>I<sub>7</sub>Cl<sub>2</sub>], (TMP = *N,N,N',N'*-tetramethyl-piperazine)<sup>15</sup> suggests that more

organic–inorganic, layered iodido bismuthates should be available if the right type of counterion can be found.

A family of organic cations that has been largely overlooked in the context of metal halide materials are iminium ions (R<sub>2</sub>C=N<sup>+</sup>R<sub>2</sub>; R = H, organic group). They are well known as reactive intermediates and reagents in organic chemistry,<sup>16</sup> but they are also known for their tendency to hydrolyze.<sup>17</sup> This reactivity suggests that they are difficult to work with in the preparation of robust materials, yet in early studies of iminium cations, halogenido metalate anions were used to isolate these species.<sup>18</sup> Later work demonstrated that compounds containing iminium cations are readily available with numerous substitution patterns<sup>19</sup> and easy to isolate as single crystals.<sup>20</sup> More recently, cuprates and argentates featuring (Me<sub>2</sub>C=NMe<sub>2</sub>)<sup>+</sup> were prepared by *in situ* condensation of dimethylamine and acetone.<sup>21</sup>

Here, we present (Me<sub>2</sub>C=NMe<sub>2</sub>)Bi<sub>2</sub>I<sub>7</sub> (**1**), a layered organic–inorganic iodido bismuthate, the first example of a layer with fully occupied metal positions in this class of compounds. We investigate the synthesis and reactivity, crystal structure and optical properties of **1**, revealing its unique topology, high stability and low band gap. We use quantum chemical methods to analyze the compound's electronic properties and demonstrate a new method to characterize and quantify iodine–iodine contacts in extended solids. We also discuss why our findings are relevant to lead halide perovskites and how the facile preparation of iminium cations opens up new opportunities for metal halide materials in general.

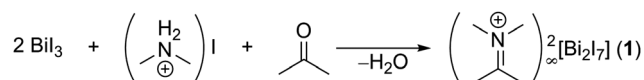
(Me<sub>2</sub>C=NMe<sub>2</sub>)Bi<sub>2</sub>I<sub>7</sub> (**1**) is obtained by heating stoichiometric amounts of BiI<sub>3</sub> and (NMe<sub>2</sub>H<sub>2</sub>)I in acetone (Scheme 1).

**1** crystallizes in *P2<sub>1</sub>/n* (No. 13) as black blocks. Fig. 1 shows an overview of the crystal structure. Bond lengths in both the cation and anion are in good agreement with literature reports

Department of Chemistry and Material Sciences Center, Philipps-Universität Marburg, Hans-Meerwein-Straße, 35043 Marburg, Germany.

E-mail: tonner@chemie.uni-marburg.de, johanna.heine@chemie.uni-marburg.de

† Electronic supplementary information (ESI) available: Synthesis, crystallographic details, thermal analysis, powder patterns, IR and Raman spectra, absorption spectra, details of computational studies. CCDC 1939881. For ESI and crystallographic data in CIF or other electronic format see DOI: 10.1039/c9cc06625j



Scheme 1 Synthesis of **1**.

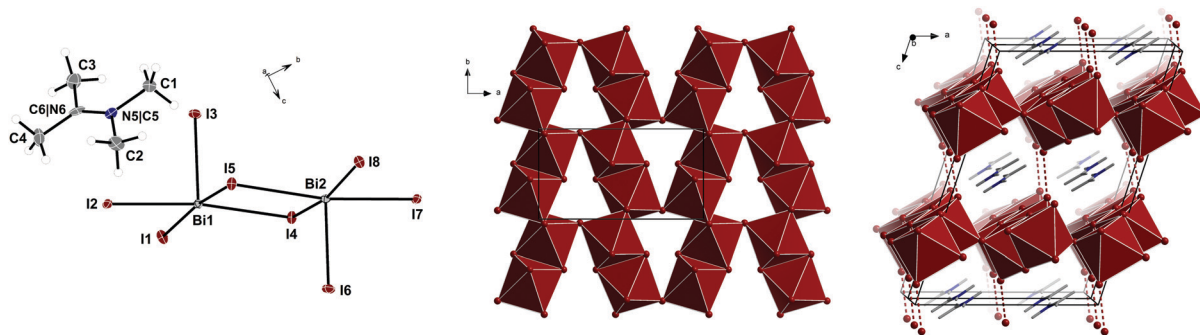


Fig. 1 Asymmetric unit of **1**, ellipsoids at 50% probability, only majority position shown (left). View along the *c* axis, cations omitted (middle). Excerpt with I–I interactions below 4 Å marked with dashed lines (right).

(Tables S3 and S4, ESI<sup>†</sup>). The iodido bismuthate layers feature the well-known motif of  $\{\text{BiI}_4\}$  chains of edge-sharing  $\{\text{BiI}_6\}$  octahedra.<sup>12</sup> These chains are connected into layers by additional edge-sharing with adjacent strands. The resulting topology is a 6<sup>3</sup>-honeycomb net. To the best of our knowledge, the anion motif found in **1** is unique among metalates, although related metal halide layers with six-membered rings are known, *e.g.* in  $\text{BiI}_3$ ,<sup>22</sup>  $(\text{pipzH}_2)\text{Mn}_2\text{F}_8$  (*pipz* = piperazine)<sup>23</sup> or the triple-layered anion in  $(\text{H}_2\text{mpz})_2\text{Pb}_3\text{Br}_{10}$  (*mpz* = 1-methylpiperazine).<sup>24</sup> The layers in **1** are further connected into a pseudo-network *via* iodine-iodine interactions.

**1** starts to decompose at 290 °C (Fig. S2, ESI<sup>†</sup>), similar to layered organic-inorganic iodido plumbates.<sup>5</sup> We also tested the stability of **1** against humidity, as the tendency of iminium cations to hydrolyze might be expected to translate to the metalate as well. However, when a powdered sample of **1** is stored in humid air for 24 h, no change in powder pattern is observed (Fig. S4, ESI<sup>†</sup>). Additionally, long term stability was investigated on a sample that was aged in air for 5 months. Here, no significant decomposition was observed in the powder diffractogram as well (Fig. S4, ESI<sup>†</sup>). The absorption spectrum of **1**, measured in diffuse reflectance, shows an onset of absorption at 1.8 eV (Fig. S7, ESI<sup>†</sup>). A comparison with the spectra of  $\text{BiI}_3$  and  $(\text{Hpy})\text{BiI}_4$ <sup>25</sup> (*Hpy* = pyridinium) highlights the effect of metalate formation and changing anion dimensionality (Fig. 2): the onset of absorption is blue-shifted going from  $\text{BiI}_3$  to **1** to  $(\text{Hpy})\text{BiI}_4$ , which features chain-like anions, as expected from general principles of dimensionality reduction in metalates.<sup>26</sup> Weller has shown that iodido bismuthate band gaps correlate not only with the anion dimensionality, but also with the presence of iodine-iodine interactions between anions, which typically lower the band gap.<sup>27</sup> We suggest that it is these interactions, also found in **1**, that cause a red-shifted onset of absorption in comparison with  $\text{Rb}_3\text{Bi}_2\text{I}_9$ , composed of (111) perovskite layers, where a band gap of 2.1 eV<sup>13</sup> has been reported and no interlayer iodine-iodine interactions below 4 Å occur. Revealing the nature of these interlayer interactions and their impact on the band gap motivated our computational investigations for **1**.

Following our previous work,<sup>28</sup> we chose density functional theory (DFT) approaches based on the PBE functional with dispersion correction by the DFT-D3 method and consideration of scalar and spin-orbit relativistic effects taking into account the

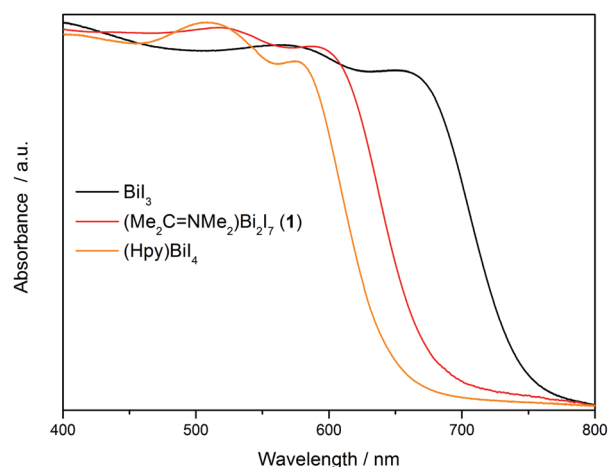


Fig. 2 Absorption spectra of  $\text{BiI}_3$ , **1** and  $(\text{Hpy})\text{BiI}_4$ , measured in diffuse reflection.

full periodicity of the system (see ESI<sup>†</sup>). The calculated band gap of 1.87 eV (TB09) is in excellent agreement with the experimental value of 1.8 eV (Table S6, ESI<sup>†</sup>). An analysis of the projected density of states (pDOS) shows that the valence band edge is mostly composed of orbitals located at the iodine atoms, while the conduction band consists of equal contributions of Bi- and I-based orbitals (Fig. 3). Plotting the orbitals at the  $\Gamma$ -point confirms these assignments in a real-space picture and demonstrates that the highest occupied crystal orbital (HOCO) consists of non-bonding electron pairs at the iodine atoms while the lowest unoccupied crystal orbital (LUCO) additionally features contributions from antibonding Bi–I orbitals. These orbitals are delocalized over the whole unit cell, indicating good carrier mobility. This picture is similar to results derived for  $\text{Rb}_3\text{Bi}_2\text{I}_9$ .<sup>13</sup> In contrast, layered lead-based perovskites typically show a higher contribution of the metal-based orbitals to the valence and conduction bands.<sup>6</sup> The interlayer interaction between the iodine atoms was previously found to be an important element for the crystal packing and electronic structure of iodido metalates.<sup>27</sup>

But the exact nature of these interactions has not been revealed up to now. Thus, we performed an in-depth analysis of the underlying principles governing the I ··· I interaction by a combination of several advanced tools for bonding analysis. In

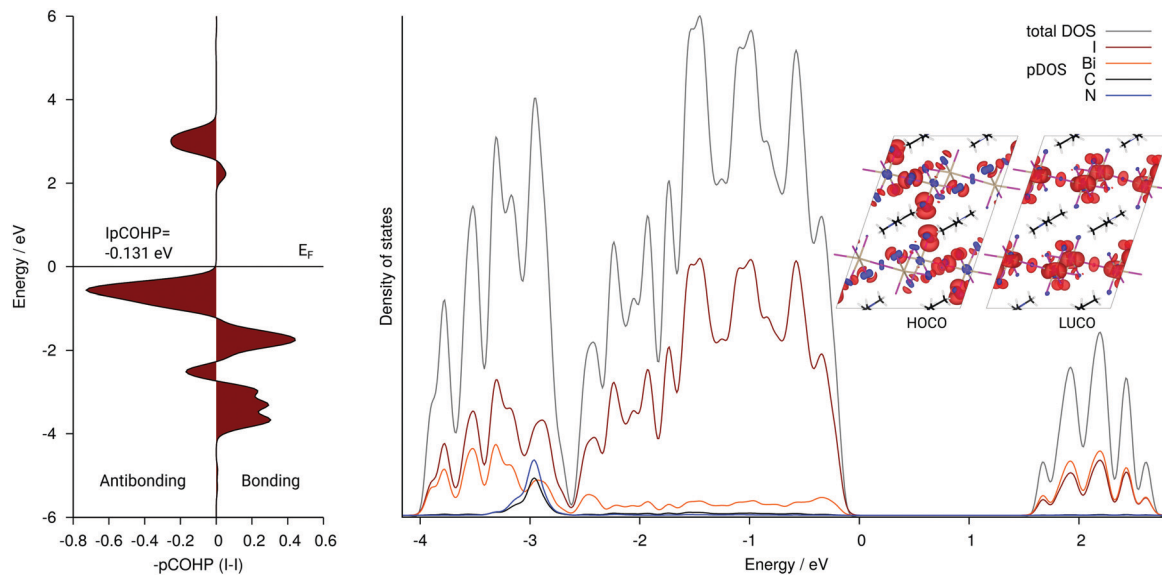


Fig. 3 Negative of the pCOHP (PBE-D3) values of the interlayer I...I interaction (left); total and partial density of states (pDOS, TB09) with insets of the highest occupied (HOCO) and lowest unoccupied crystal orbital (LUCO) at the  $\Gamma$ -point (right).

Fig. 3, we show the projected Crystal Orbital Hamilton Population (pCOHP<sup>29</sup>) of the I...I interaction. In agreement with the results from the pDOS analysis, an antibonding contribution stemming from non-bonding electron pair repulsion is found close to the Fermi energy. The integrated pCOHP (IpCOHP) amounts to  $-0.131$  eV indicating an overall slightly attractive interaction. The topological analysis by the atoms in molecules (AIM) method<sup>30</sup> shows an increased but small electron density at the bond critical points for the interlayer I...I interactions compared to the intralayer contacts and a positive value for the second derivative of the electron density (Laplacian,  $\nabla^2\rho$ ) supporting the notion of a non-covalent interaction (Table S7, ESI<sup>†</sup>).

A quantitative analysis of this interaction was carried out with our recently developed energy decomposition analysis for extended systems (pEDA). This analysis decomposes the bonding energy between two fragments in terms of well-defined energy contributions that help to gain a qualitative understanding of the bonding interaction from quantitative results. It is thus possible to distinguish effects from quasiclassical electrostatic interactions ( $\Delta E_{\text{elstat}}$ ), Pauli repulsion ( $\Delta E_{\text{Pauli}}$ ) and orbital interactions ( $\Delta E_{\text{orb}}$ ). Dispersion contributions to the bonding are derived from the DFT-D3 scheme ( $\Delta E_{\text{int}}(\text{disp})$ ) and added to the sum of the electronic interaction terms ( $\Delta E_{\text{int}}(\text{elec})$ ) to give the total interaction energy ( $\Delta E_{\text{int}}$ ).<sup>31–33</sup> Notably, the layered structure of **1** enables an analysis of a 3-dimensional solid not composed of molecular units with an EDA method for the first time, since commonly a reasonable fragmentation is not possible. Here, the fragmentation is done by including one layer of organic and inorganic component each as sketched in Fig. S8a (ESI<sup>†</sup>) to form a double layer as one fragment. The pEDA results for **1** are summarized in Table S8 (ESI<sup>†</sup>). Surprisingly, the interaction energy between these double layers stems nearly equally from dispersion (53%) and electronic (47%) contributions indicating a more complex situation than pure van-der-Waals binding. A further

look into the attractive pEDA terms shows that the electrostatic interaction is dominating (56%) which can be understood by the ionic nature of the organic and inorganic layers, respectively. Nevertheless, a significant orbital interaction (44%) is found, indicating covalent bonding contributions. These orbital interactions were further analyzed with the Natural Orbitals for Chemical Valence (NOCV) approach,<sup>33,34</sup> identifying iodine–iodine charge shift as the major contribution (Fig. S8 and S9, ESI<sup>†</sup>).

But how does this I–I interaction effect the band edges? To this end we reduced this interaction by increasing the interlayer I–I distance from 3.692 to 4.047 Å (9.6%) while keeping the other structural parameters constant. A pCOHP analysis (Fig. S10, ESI<sup>†</sup>) reveals that the antibonding contribution close to the Fermi energy decreases more than its bonding counterparts leading to a decreased IpCOHP of  $-0.051$  eV. In addition, the HOCO is shifted to slightly lower energies ( $-0.1$  eV). This shows that the interlayer I...I interaction leads to a smaller band gap, implying the possibility of band gap tuning by controlling the iodine–iodine distances.

We want to highlight another aspect of our findings: the facile synthesis and inclusion of the iminium cations in **1**, and its relevance to the synthesis of metal halide perovskites. Dimethylformamide, a common solvent in metal halide perovskite synthesis, can form dimethylamine as a decomposition product<sup>35</sup> and subsequently  $(\text{NMe}_2\text{H}_2)^+$  cations in the presence of acids, a phenomenon that has already been observed in  $\text{CsPbI}_3$  perovskites.<sup>36</sup> Our results indicate that a further reaction towards iminium cations may occur when ketones are added to the reaction mixture, for example during the synthesis of nanoparticles.<sup>37</sup> The partial inclusion of larger organic cations in lead halide perovskites does not necessarily change the crystal structure, but can have significant effects on optical properties and stability.<sup>38</sup> While this may occur accidentally, it can also be used deliberately to tune the properties of mixed

cation perovskite materials.<sup>39</sup> On a broader scope, the wide range of possible starting materials for iminium ions – amines and ketones or aldehydes – allows for targeting specific cation sizes and shapes that were previously unavailable and may yield unique new anion topologies and material properties, not only for halogenido bismuthates, but metalates in general.

In summary, we show that layered organic–inorganic iodido bismuthates are available given the right cation:  $(\text{Me}_2\text{C}=\text{NMe}_2)\text{Bi}_2\text{I}_7$  combines a simple synthetic access with a layered anion topology, low band gap and good stability and thus holds great promise for material applications. Our computational investigations show a band gap in good agreement with experiment and characterize it as a  $\text{I} \rightarrow \sigma^*(\text{Bi}-\text{I})$  transition. Using energy decomposition analysis for the first time in an inorganic 3D system, we quantitatively and qualitatively elucidate the  $\text{I} \cdots \text{I}$  interactions found as structural elements with dispersion interactions and polarization of the iodine atoms as the major bonding contributions. Our results highlight iminium cations as prime counterion templating candidates for new metalate materials with unprecedented anion topologies.

This work is funded by the DFG via the SFB 1083. J. H. thanks Prof. Stefanie Dehnen for her constant support. N. D. thanks the Fonds der Chemischen Industrie and the Studienstiftung des Deutschen Volkes for their support. We thank the HLR Stuttgart, HRZ Marburg, and Goethe-HLR Frankfurt for computational resources, Jakob Möbs for preparing reference compounds, Dr Istemi Kuzu for recording the Raman spectrum and Dr Robert Wilson for helpful discussions.

## Conflicts of interest

There are no conflicts to declare.

## References

- C. C. Stoumpos and M. G. Kanatzidis, *Adv. Mater.*, 2016, **28**, 5778–5793.
- A. K. Jena, A. Kulkarni and T. Miyasaka, *Chem. Rev.*, 2019, **119**, 3036–3103.
- X. Zhu, Y. Lin, Y. Sun, M. C. Beard and Y. Yan, *J. Am. Chem. Soc.*, 2019, **141**, 733–738.
- L. N. Quan, B. P. Rand, R. H. Friend, S. G. Mhaisalkar, T.-W. Lee and E. H. Sargent, *Chem. Rev.*, 2019, **119**, 7444–7477.
- D. B. Mitzi, *Chem. Mater.*, 1996, **8**, 791–800.
- C. C. Stoumpos, D. H. Cao, D. J. Clark, J. Young, J. M. Rondinelli, J. I. Jang, J. T. Hupp and M. G. Kanatzidis, *Chem. Mater.*, 2016, **28**, 2852–2867.
- L. Mao, C. C. Stoumpos and M. G. Kanatzidis, *J. Am. Chem. Soc.*, 2019, **141**, 1171–1190.
- H. Li, R. Wang and H. Sun, *Acc. Chem. Res.*, 2019, **52**, 216–227.
- K. Eckhardt, V. Bon, J. Getzschmann, J. Grothe, F. M. Wisser and S. Kaskel, *Chem. Commun.*, 2016, **52**, 3058–3060.
- S. M. Jain, D. Phuyal, M. L. Davies, M. Li, B. Philippe, C. De Castro, Z. Qiu, J. Kim, T. Watson, W. C. Tsoi, O. Karis, H. Rensmo, G. Boschloo, T. Edvinsson and J. R. Durrant, *Nano Energy*, 2018, **49**, 614–624.
- M. A. Green, Y. Hishikawa, E. D. Dunlop, D. H. Levi, J. Hohl-Ebinger, M. Yoshita and A. W. Y. Ho-Baillie, *Prog. Photovolt. Res. Appl.*, 2019, **27**, 3–12.
- N. Mercier, N. Louvain and W. Bi, *CrystEngComm*, 2009, **11**, 720–734.
- A. J. Lehner, D. H. Fabini, H. A. Evans, C.-A. Hébert, S. R. Smock, J. Hu, H. Wang, J. W. Zwanziger, M. L. Chabinye and R. Seshadri, *Chem. Mater.*, 2015, **27**, 7137–7148.
- D. B. Mitzi, *Inorg. Chem.*, 2000, **39**, 6107–6113.
- M.-Q. Li, Y.-Q. Hu, L.-Y. Bi, H.-L. Zhang, Y. Wang and Y.-Z. Zheng, *Chem. Mater.*, 2017, **29**, 5463–5467.
- A. Erkkilä, I. Majander and P. M. Pihko, *Chem. Rev.*, 2007, **107**, 5416–5470.
- H. G. Reiber and T. D. Stewart, *J. Am. Chem. Soc.*, 1940, **62**, 3026–3030.
- M. Lamchen, W. Pugh and A. M. Stephen, *J. Chem. Soc.*, 1954, 4418–4425.
- N. J. Leonard and J. V. Paukstelis, *J. Org. Chem.*, 1963, **28**, 3021–3024.
- L. M. Trefonas, R. L. Flurry Jr., R. Majeste, E. A. Meyers and R. F. Copeland, *J. Am. Chem. Soc.*, 1966, **88**, 2145–2149.
- R. Hehl and G. Thiele, *Z. Anorg. Allg. Chem.*, 2000, **626**, 2167–2172.
- M. Ruck, *Z. Kristallogr.*, 1995, **210**, 650–655.
- R. Stief and W. Massa, *Z. Anorg. Allg. Chem.*, 2006, **632**, 797–800.
- L. Mao, P. Guo, M. Kepenekian, I. Hadar, C. Katan, J. Even, R. D. Schaller, C. C. Stoumpos and M. G. Kanatzidis, *J. Am. Chem. Soc.*, 2018, **140**, 13078–13088.
- T. Li, Y. Hu, C. A. Morrison, W. Wu, H. Han and N. Robertson, *Sustainable Energy Fuels*, 2017, **1**, 308–316.
- E. G. Tulskey and J. R. Long, *Chem. Mater.*, 2001, **13**, 1149–1166.
- A. J. Dennington and M. T. Weller, *Dalton Trans.*, 2018, **47**, 3469–3484.
- N. Dehnhardt, H. Borkowski, J. Schepp, R. Tonner and J. Heine, *Inorg. Chem.*, 2018, **57**, 633–640.
- R. Dronskowski and P. E. Blöchl, *J. Phys. Chem.*, 1993, **97**, 8617–8624.
- R. F. W. Bader, *Chem. Rev.*, 1991, **91**, 893–928.
- Dispersion interactions are of course electronic in origin as well. Distinguishing them from the electrostatic and overlap-based terms in the pEDA nevertheless gives us additional insight into the nature of the chemical bond.
- M. Raupach and R. Tonner, *J. Chem. Phys.*, 2015, **142**, 194105.
- L. Pecher and R. Tonner, *Wiley Interdiscip. Rev.: Comput. Mol. Sci.*, 2018, e1401.
- M. P. Mitoraj, A. Michalak and T. Ziegler, *J. Chem. Theory Comput.*, 2009, **5**, 962–975.
- S. Ding and N. Jiao, *Angew. Chem., Int. Ed.*, 2012, **51**, 9226–9237.
- W. Ke, I. Spanopoulos, C. C. Stoumpos and M. G. Kanatzidis, *Nat. Commun.*, 2018, **9**, 4785.
- Q. A. Akkerman, S. G. Motti, A. R. S. Kandada, E. Mosconi, V. D'Innocenzo, G. Bertoni, S. Marras, B. A. Kamino, L. Miranda, F. De Angelis, A. Petrozza, M. Prato and L. Manna, *J. Am. Chem. Soc.*, 2016, **138**, 1010–1016.
- I. Spanopoulos, W. Ke, C. C. Stoumpos, E. C. Schueller, O. Y. Kontsevoi, R. Seshadri and M. G. Kanatzidis, *J. Am. Chem. Soc.*, 2018, **140**, 5728–5742.
- W. Ke, I. Spanopoulos, Q. Tu, I. Hadar, X. Li, G. S. Shekhawat, V. P. Dravid and M. G. Kanatzidis, *J. Am. Chem. Soc.*, 2019, **141**, 8627–8637.